Multi-Spectral Cloud Property Retrieval

B. E. Carlson
National Aeronautics and Space Administration
Goddard Institute for Space Studies
New York, New York

R. Lynch
Atmospheric and Environmental Research, Inc.
Cambridge, Massachusetts

Introduction

Despite numerous studies to retrieve cloud properties using infrared measurements the information content of the data has not yet been fully exploited. Nonetheless, infrared retrievals provide the best means to examine diurnal variations in cloud properties as well as to examine seasonal changes at high latitudes. Thermal infrared brightness temperature (T_b) difference techniques, such as the split-window (Inoue 1985; Prabhakara et al. 1988) and the tri-spectral (Ackerman et al. 1990; Strabala et al. 1994), have been used for years to estimate the optical depth (τ) and/or effective radius (r_{eff}) of cirrus. These techniques utilize the spectral dependence of cloud optical properties and the non-linearity of the Planck function to detect clouds and retrieve their radiative properties. The sensitivity of these retrievals to inaccurate estimates of the cloud temperature, cloud inhomogeneity, surface properties, and cloud particle shape have been investigated.

In an effort to more fully utilize the information content of the infrared measurements, we have developed a multi-spectral technique for retrieving phase, effective cloud particle size, optical depth, and effective cloud temperature. While this technique is applicable to all cloud types, we begin with a retrieval of cirrus cloud properties.

Observations

In this investigation we analyze the data from the High resolution Interferometer Sounder (HIS) and validate our results using the data from cloud and aerosol LIDAR system (CLS) and the MAS (MODIS [Moderate-Resolution Imaging Spectroradiometer] Airborne Simulator). The HIS (Smith et al. 1995) is a Michelson interferometer covering a broad spectral region of the infrared (3.5 µm to 19 µm) with a high spectral resolution ($\lambda/\Delta\lambda > 2000$) and a spatial resolution of 2 km at the earth's surface below the ER-2 at 20 km. The MAS (King et al. 1996) consists of 50 spectral channels (0.55 µm to 14.2 µm) scanning contiguously a swath 40-km wide beneath the ER-2 with a spatial resolution of 50 m at a flight altitude of 20 km. The CLS uses a Nd:YAG-laser operating at 0.532 µm to provide cloud top altitudes and the thicknesses of the optically thin clouds beneath the ER-2 aircraft. Thus, while these instruments

are collocated on the ER-2 platform their fields of view are different and MAS measurements are needed to investigate the discrepancies between the CLS and HIS measurements. In particular, the CLS measurements cannot be used to identify "clear" HIS scenes.

The cirrus in this study were observed on April 20, 1996, as part of the Subsonic aircraft Contrail and Cloud Effects Special Study (SUCCESS). The ER-2 flew in the vicinity of the CART (Clouds and Radiation Testbed) site in northern Oklahoma. To ensure uniform viewing geometry we have eliminated the data obtained during aircraft turns and analyze the data from the straight flight segments.

We chose the measurements from the April 20, 1996, because, as shown in Figure 1, the CLS data indicate that the field of view of the HIS instrument was dominated by high level single- and closely spaced multi-level cirrus. The CLS data indicate that the clouds were typically located between 7 km and 10 km. Although the CLS receives a return signal from the ground throughout most of this flight, indicative of optically thin clouds, there are some times, particularly around 18:00:00 Universal Time Coordinates (UTC) where the clouds become optically thick (i.e., no return from the ground). Also, clear regions were observed throughout the flight ensuring clear-sky references reasonably close in space and time to each of the cloudy sky spectra. Since the measurements were obtained over the CART site there exists a large amount of correlative data, such as sonde data. Finally, other researchers have analyzed data for this day allowing us to compare our results with theirs.
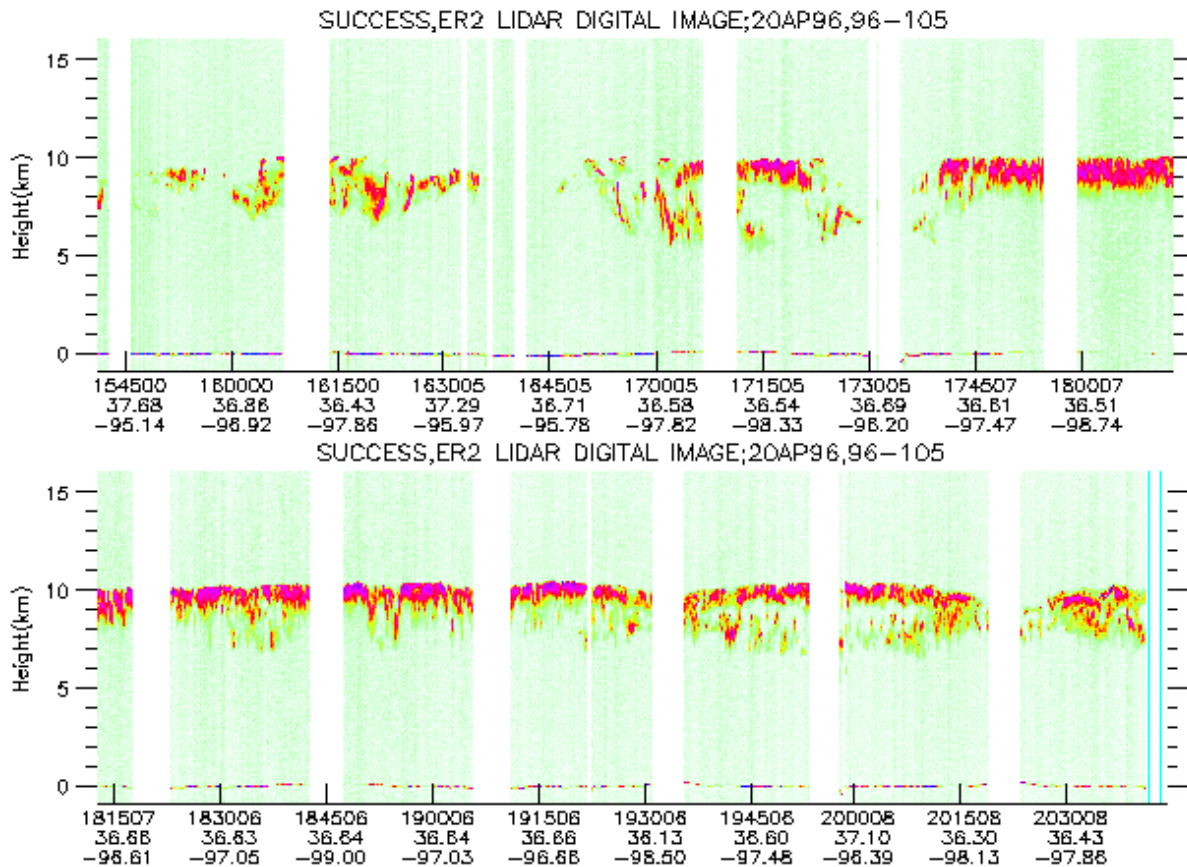
Figure 1. CLS backscatter cross section as a function of height and time for April 20, 1996.

Method

We have developed an objective algorithm that first classifies the HIS spectra as either cloudy or clear based on the degree to which the spectrum deviates from Planck. We then impose an additional radiance threshold and select the three hottest "clear" spectra to obtain the clear-sky reference spectrum. Since we are, in effect, using a brightness temperature threshold, we partition the data into four separate time intervals to account for diurnal heating from morning to afternoon.

We retrieve the cloud properties using measurements in the 8-μm, 10-μm, and 12-μm regions and evaluate the quality of the retrieval by comparing the observed and modeled radiances in six spectral bands. Within each spectral band, denoted with the subscript ν, the radiative transfer equation can be written as:

$$R_{cld\nu} = R_{clr\nu} + T_\nu(r_{eff},\tau) + B_\nu(T_c)\varepsilon_\nu(r_{eff},\tau) \tag{1}$$

where R_{cld} and R_{clr} are the observed cloudy and local clear-sky radiances averaged over the band and T and ε are the transmissivity and emissivity of the cloud, respectively. These terms depend on effective radius r_{eff} and optical depth τ. B_ν is the Planck function which depends on the temperature of the cloud T_c.

By combining equations for band pairs, with the band in the 12-μm region used in both band pairs, we can eliminate T_c and define the function F such that

$$F = [R_{cld\nu1} - R_{clr\nu2}\,T_{\nu1} + a_{\nu1}{}^3\varepsilon] \times (R_{clr\nu2} - R_{clr\nu2}\,T_{\nu2})^w - [R_{cld\nu1} - R_{clr\nu2}\,T_{\nu1}] \times (R_{clr\nu2} - R_{clr\nu2}\,T_{\nu2} + a_{\nu2}{}^3\varepsilon)^w \tag{2}$$

where $w = \nu_1/\nu_2$ and $\nu_1 < \nu_2$.

For each band pair, the coupled equations are solved for τ using look-up tables for the transmissivity and emissivity calculated as functions of particle size and optical depth. Calculations were performed for 98 particle sizes ranging from 1 μm to 50 μm and 300 optical depths (referenced at 0.5 μm) the log of which varies from -1.5 to 1.5 for both water and ice. Mie theory is used to account for the spectral dependence particle extinction assuming a gamma size distribution with an effective variance of 0.25. Multiple scattering calculations were performed using the doubling-adding method and a Henyey-Greenstein phase function.

For each r_{eff} an optical depth is determined such that F=0. Thus, we generate a curve in (r_{eff},τ) space. This procedure is repeated for another pair of bands generating another curve in (r_{eff},τ) space. Since we require that the solution fits all wavelengths, the intersection of the curves determines r_{eff} and τ. Substituting these values into the Eq. (1) allows us to solve for T_c. If the curves never cross in (r_{eff},τ) space, then no fit is obtained and these spectra are labeled "no fit." In addition, it is possible to obtain an ice fit with a cloud temperature in excess of 273°K (clearly indicative of a water cloud) or a water fit with a cloud temperature significantly below the freezing point of water. Such a fit would be labeled "anomalous." Having failed to fit some of the spectra assuming that the cloud fills the field of view, the

algorithm considers broken cloudiness by decreasing the cloud fraction within the HIS field of view and repeating the fitting procedure using a mixture of clear and cloudy skies to calculate the radiance.

Results

Here we present the results of our analysis of 1286 HIS spectra obtained on April 20, 1996. Of these, 971 were identified to contain cirrus clouds, 157 spectra were identified as clear sky, and 158 of the spectra had fits that were anomalous (retrieved phase and effective temperature disagree). As shown in Figure 2 our retrieved optical depths range from about 0.1 to almost 12.0 with an average value of 1.8. Our retrieved particle sizes range from 15 µm to 30 µm with an average value of 21.1 µm and a standard deviation of 3.3 µm. Our retrieved cloud temperatures (not shown) range from 170°K to 280°K with the majority of the retrieved cloud temperatures falling between 215°K and 245°K with an average temperature of 233°K.

We use the vertical profiles of temperature from the conventional sondes in combination with the CLS data to determine the temperature range of the CLS detected clouds for comparison with our retrieval results. Figure 3 shows the results of combining the sonde measurements at 1730 UTC and 2030 UTC with the CLS backscatter cross section. Here, we see that the CLS-detected clouds are located in the temperature range between 215°K and 245°K.

While the bulk of our retrieved cloud temperatures fall within the CLS-sonde range, there are, however, cases where the retrieved values falls outside this range. Based on comparison with the CLS data, we find that the accuracy of our T_c retrieval depends on the optical depth of the cloud and whether or not multiple cloud layers are present.   For optically thick clouds, our retrieved cloud temperature corresponds to the CLS values. In the presence of multiple, thin cloud layers, the retrieved cloud temperature is within the range of the CLS-detected layers.
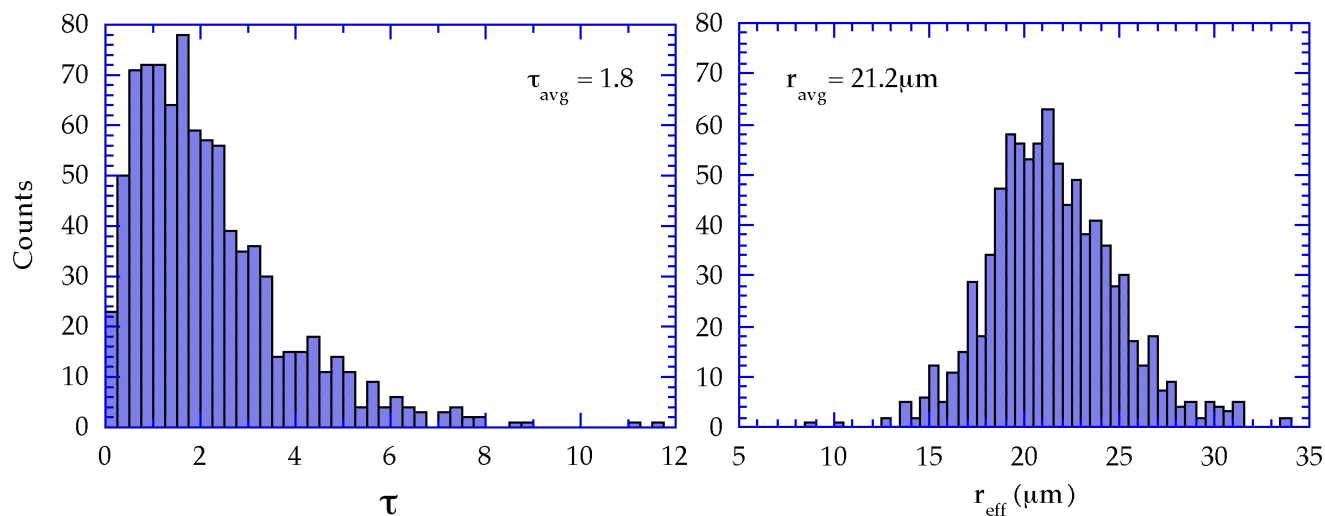
Figure 2. Histogram of retrieved cloud optical depth (left) and retrieved cloud effective radius (right).
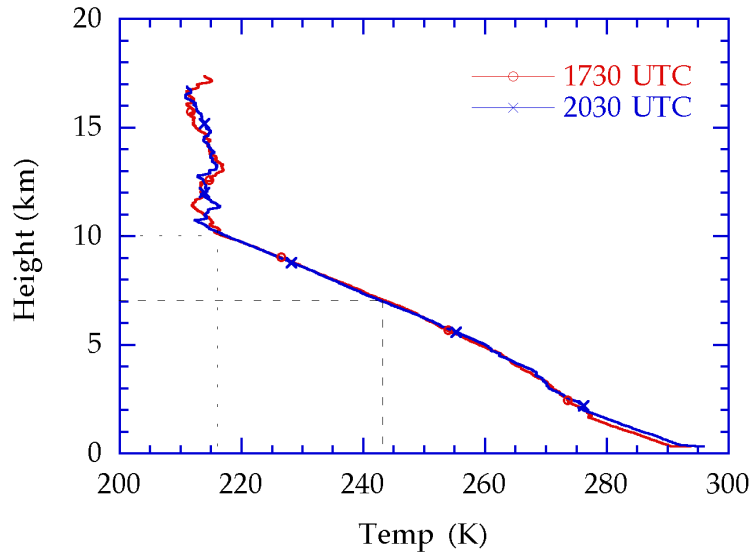
Figure 3. Temperature profile from the 1730 UTC and 2030 UTC sonde measurements combined with the CLS-determined cloud height boundaries.

Figure 4 shows the relationship between the observed 11-µm brightness temperature and the retrieved cloud temperature for three optical depth ranges. Here we see that while the bulk of the retrieved cloud temperatures fall within the CLS-sonde range, a significant fraction of the retrieved cloud temperatures fall outside this range. Moreover, we see a larger variation in retrieved cloud temperature associated with optically thin clouds.
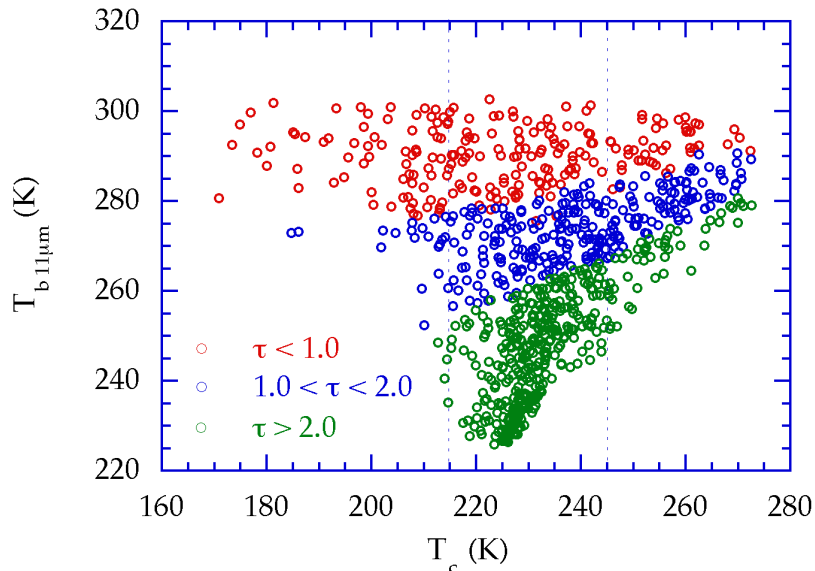
Figure 4.   Relationship between the observed 11-µm brightness temperature and retrieved cloud temperature for several optical depth ranges.

Discussion

Duda et al. (1998) analyzed the MAS data of two contrails (1556 UTC and 1634 UTC) on this day. While no corresponding HIS measurements exist for the first contrail, we can compare our results with theirs for the older contrail that was observed at 1634 UTC. For this contrail, Duda et al. report optical depths ranging from near zero to over 1.5 in good agreement with the optical depths retrieved from the coincident HIS spectra. While their optical depths retrieved from the 8.5 µm to 11 µm and 11 µm to 12 µm brightness temperature differences are nearly identical, the particle sizes retrieved by modeling the 8.5 µm to 11 µm brightness temperature differences are larger (mean radius: 27.3 µm) than their 11 µm to 12 µm counterparts (mean radius: 18.2 µm). Moreover, they find that they are also more variable (standard deviation of 7.7 µm versus 6.0 µm). Since older contrails, such as the one observed at 1634 UTC, have optical properties that resemble the surrounding cirrus it is perhaps not surprising that our average radius (21.2 µm) falls within their retrieved values.

Given that the bulk of our retrieved particle sizes, optical depths, and cloud temperatures are in excellent agreement with correlative measurements, it is troubling that there is such a large variation in the retrieved cloud properties for low optical depth cases. To further examine this, we have taken a more careful look at our retrieval results. We find significant changes in the cirrus with time along the flight track. The interval from 1518 UTC to 1607 UTC contains 167 HIS spectra. The algorithm does not find a fit for 84 of these spectra. In addition we retrieve anomalous fits for 45 of the spectra. Only 39 of these spectra are identified as cirrus with an average optical depth of 1.2, an average r_{eff} of 17.6 µm and an average cloud temperature of 235.8°K. The most interesting result is that the average cloud fraction is 0.65. The interval from 1609 UTC to 1706 UTC contains 214 spectra. For these spectra, we retrieved 41 no fits, 48 anomalous fits and 125 cirrus retrievals with an average optical depth of 1.37, an average r_{eff} of 19.5 µm and an average effective cloud temperature of 243.4°K. The average cloud fraction is 0.85. The interval from 1711 to 1842 contains 399 spectra. For these spectra, we retrieved 15 no fits, 49 anomalous fits, and 335 cirrus fits with an average optical 2.7, an average r_{eff} of 19.7 µm, and an average cloud temperature of 237°K. The retrieved cloud fraction is 0.98. The final interval, from 1846 UTC to 2039 UTC contains 505 spectra. For these spectra, we retrieved 17 no fits, 16 anomalous fits, and 472 cirrus fits with an average optical depth of 1.4, an average r_{eff} of 20.8 µm, an average cloud temperature of 229.6°K, and an average cloud fraction of 0.97. These results suggest that for the first two time intervals, the cirrus were spatially inhomogeneous/broken within the HIS field of view. Thus, we find that the current quality of our retrieval depends on the degree with which the cloud fills the field of view. This notion is confirmed by examining the CLS data, shown previously in Figure 1, which indicate that the cirrus were more tenuous and broken in the interval 1545 UTC to 1615 UTC. The MAS data are also consistent with this interpretation. As the next step in this investigation, we will perform a correlative analysis of the MAS measurements within the HIS fields of view and the HIS data to improve the quality of the retrieval in the presence of broken cloudiness.

References

Ackerman, S. A., W. L. Smith, J, D. Spinhirne, and H. E. Revercomb, 1990: The 27-28 October 1986 FIRE IFO cirrus case study: Spectral properties of cirrus clouds in the 8-12 μm window. *Mon. Weather Rev.*, **118**, 2377-2388.

Duda, D. P., J. D. Spinhirne, and W. D. Hart, 1998: Retrieval of contrail microphysical properties during SUCCESS by the split-window method. *Geophys. Res. Lett.*, **25**, 1149-1152.

Inoue, T., 1985: On the temperature and effective emissivity determination of semitransparent cirrus clouds by bispectral measurements in the 10 μm window region. *J. Meteorol. Soc. Japan*, **63**, 88-98.

King, M. D., W. P. Menzel, P. S. Grant, J. S. Myers, G. T. Arnold, S. E. Platnick, L. E. Gumley, S.-C. Tsay, C. C. Moeller, M. Fitzgerald, K. S. Brown, and F. G. Osterwich, 1996: Airborne scanning spectrometer for remote sensing of cloud, aerosol, water vapor, and surface properties. *J. Atmos. Oceanic Technol.*, **13**, 777-794.

Prabhakara, C., R. S. Fraser, G. Dalu, M. L. C. Wu, R. J. Curran, and T. Styles, 1988: Thin cirrus clouds: Seasonal distribution over oceans deduced from Nimbus-4 IRIS. *J. Appl. Meteor.*, **27**, 379-399.

Smith, W. L., H. E. Revercomb, R. P. Knuteson, F. A. Best, R. Dedecker, H. B. Howell, and H. M. Woolf, 1995: Cirrus cloud properties derived from high spectral resolution infrared spectrometry during FIRE II. Part I: The High resolution Interferometer Sounder (HIS) Systems. *J. Atmos. Sci.*, **52**, 4238-4245.

Strabala, K. I., S. A. Ackerman, and W. P. Menzel, 1994: Cloud properties inferred from 8-12 μm data. *J. Appl. Meteor.,* **2**, 212-229.